Trehalose Transport Dynamics Underpin a Metabolic Trade-Off between Exogenous Uptake and Endogenous Synthesis in Lepidopteran Insects

Bhagyashri Y. Chaudhari[1, 2*] , Vikram J. Nichit[1, 2*], Vitthal T. Barvkar[3], Rakesh Shamsunder Joshi[1, 2*]

[1]Biochemical Sciences Division, CSIR-National Chemical Laboratory, Dr. Homi Bhabha Road, Pune, 411008, Maharashtra, India

[2]Academy of Scientific and Innovative Research (AcSIR), Ghaziabad 201002, Uttar Pradesh, India

[3]Department of Botany, Savitribai Phule Pune University, Pune, 411007, Maharashtra, India

***Corresponding author**

Dr. Rakesh Shamsunder Joshi

Biochemical Sciences Division, CSIR – National Chemical Laboratory

Dr. Homi Bhabha Road, Pune – 411 008, INDIA

Email: rs.joshi@ncl.res.in

Tel (office): 020-2590-2247

Abstract

Trehalose is the major insect hemolymph sugar and plays a diverse role. Its level is regulated endogenously by the dynamics of biosynthesis and distribution by sugar transporters (STs). The metabolic trade-off between trehalose synthesis and uptake remains poorly understood, despite its critical role in homeostasis. Here, we examined the role of a gut-specific trehalose transporter, *HaST46*, in regulating this metabolic trade-off in *Helicoverpa armigera*, a Lepidopteran pest model. Integrated transcriptomics analysis and functional analyses revealed that *HaST46* acts as a diet-responsive transporter, localised to the posterior midgut, with trehalose preference. Its expression is modulated in response to dietary trehalose availability, enhancing the efficient exogenous trehalose uptake while attenuating its endogenous synthesis and conserving energy. Functional perturbation through overexpression and silencing revealed a feedback-regulated mechanism in which *HaST46* expression showed strong correlation with trehalose metabolising enzymes and other HaSTs isoforms to maintain systemic trehalose homeostasis. Overall, our findings reveal a metabolic trade-off between exogenous trehalose uptake and endogenous synthesis mediated by gut-specific sugar transporters.

Keywords: Trehalose, Sugar uptake, Metabolism, Transporters, *Helicoverpa armigera*, Gut

1. Introduction

Insects exhibit a remarkable metabolic adaptation that contributes to their ecological success. Carbohydrates serve as a primary energy source for fuelling flight, development, reproduction, diapause, and stress tolerance (Thorat et al. 2012; Feofilova et al. 2014). Under stress conditions, insects must precisely regulate their energy acquisition, storage, and mobilisation (Zhang et al. 2019). Trehalose is the predominant hemolymph sugar in insects, fulfilling both structural and metabolic functions (Becker et al. 1996; Matsushita and Nishimura 2020; Nishimura 2020; Murphy and Wyatt 1965; Shukla et al. 2015). Its transport and metabolism are essential for insect growth and adaptability (Tellis, Kotkar, et al. 2023). Trehalose is primarily synthesised in the fat body through a conserved pathway involving *trehalose-6-phosphate synthase* (*TPS*) and *trehalose-6-phosphate phosphatase* (*TPP*) (Murphy and Wyatt 1965; Becker et al. 1996). Following synthesis, trehalose is transported into the hemolymph and then distributed to the target tissues as per the energy demand through trehalose transporters (TRETs) (Tellis, Chaudhari, et al. 2023).

Insects can ingest a wide range of foods to obtain complementary nutrients during nutritional scarcity (Koyama et al. 2020; Raubenheimer and Jones 2006). They further optimise energy utilization through metabolic balancing, enabling adaptation to diverse dietary conditions (Smith et al. 2018; Chown and Gaston 1999). Trehalose synthesis requires a continuous supply of ATP and carbon skeletons from glycolysis, glycogenolysis, or gluconeogenesis (Miyamoto and Amrein 2017). Depending on resource availability, resource insects may shift their metabolism to suppress endogenous synthesis and prioritise exogenous uptake (Izadi 2025). Hemolymph trehalose levels range from 5 to 50mM, which is maintained by continuous exchange

via TRETs for effective utilisation (Thompson 2003;,Al Hinai et al. 2025;,Wyatt 1967; Kikawada et al. 2007). TRETs are key in regulating metabolic trade-offs under controlled and stressed conditions (Leyria et al. 2020). The midgut is the primary site of sugar and nutrient absorption, detoxification, and enzymatic activity (Huang et al. 2015). To meet the metabolic demand, insects rely on sugar transporters such as TRETs, sodium-glucose co-transporters (SGLTs), and facilitative glucose transporters (GLUTs) to manage dietary sugar acquisition and use (Chaudhari et al. 2025).

Phytophagous insects such as *H. armigera* can acquire trehalose directly from their diet (Shukla et al. 2015; Tellis, Kotkar, et al. 2023). In *H. armigera*, trehalose-specific sugar transporters (*HaSTs*) showed diversity and spatio-temporal expression patterns (Tellis, Chaudhari, et al. 2023). In dipteran and hymenopteran insects, glucose absorption is primarily mediated by SGLTs. and GLUTs (Wang et al. 2016). In *Drosophila melanogaster,* the diet-responsive GLUT homolog CG4797 and SGLT homolog dSGLT1 have been shown to influence development, fertility, and survival (Chaudhari et al. 2025). The activity of these transporters is closely linked to the insulin and TOR signalling pathways, facilitating metabolic plasticity by coupling nutrient availability with growth regulation (Riera et al. 2016). This critical trait allows insects to cope with environmental stressors, shift between trophic modes, and optimise energy expenditure during metamorphosis or overwintering (Danks 2007). The interplay between trehalose metabolism and other physiological systems, including neuroendocrine signalling, symbiotic relationships, and hormonal regulation, facilitates nutrient sensing, energy homeostasis, and ecological adaptability (Tellis, Kotkar, et al. 2023).

83 Despite advances in understanding trehalose metabolism within insects, the
84 integrated dynamics between endogenous trehalose synthesis and exogenous uptake
85 remain poorly understood in many model and non-model organisms. Lepidopteran
86 pests such as *H. armigera* serve as valuable models for metabolic studies due to their
87 high dietary adaptability, rapid development, and stress resilience (Riaz et al. 2021).
88 Elucidating how these insects regulate trehalose metabolism in response to diet offers
89 insights into the metabolic homeostasis and its impact on physiological processes
90 (Dawkar et al. 2016; Guan et al. 2024; Tian et al. 2025; Zhou et al. 2023). Here, we
91 shed light on the functional role of the trehalose transporter, *HaST46,* in mediating the
92 metabolic trade-off between trehalose's exogenous uptake and endogenous
93 synthesis. Through differential gene expression analysis, qRT-PCR, LC-MS-based
94 metabolomics, enzyme activity assays, and genetic manipulation, we investigated how
95 dietary trehalose influences *HaSTs* dynamics and activity, mainly in the gut. This study
96 advances the knowledge of sugar transport, metabolic homeostasis and nutritional
97 physiology.

98 **2. Results**

99 **2.1. *HaST46* showed posterior midgut-specific expression at the transcript and**
100 **protein levels**

101 We analyzed the gut-specific expression and proteomic presence of selected putative
102 trehalose transporters, *HaSTs*, using publicly available *H. armigera* transcriptomic and
103 proteomic datasets (Ioannidis et al. 2022). Our previous study elucidated five putative
104 trehalose transporters with selective abundance in specific tissues, among which
105 *HaST46* and *HaST69* were found to be present in gut-specific transcriptomic data
106 **(Figure 1a)**. While only *HaST46* showed expression in proteomic data, indicating its

107 proteomic level abundance in the mid-gut **(Figure 1b)**. In the transcriptomics dataset,
108 *HaST46* and *HaST69* showed high expression levels across larval stages (L2, L3, L4)
109 and in different gut regions, including foregut (FG), anterior midgut (AMG), middle
110 midgut (MMG), posterior midgut (PMG), and hindgut (HG) in fifth instar (L5) larvae.
111 *HaST46* expression peaked in the gut during the L4 larval stage and in the PMG of L5
112 larvae **(Figure 1a)**. Given that feeding activity peaks during the fourth and fifth larval
113 instars, elevated expression of the sugar transporter likely supports increased
114 metabolic demand. Collectively, these data highlight that *HaST46* is a putative key
115 facilitator of sugar transport across the PMG during the energetically demanding
116 developmental stages and the period of active feeding. Transcriptomics comparisons
117 were conducted between the gut compartments of L5 larvae fed an artificial diet (AD)
118 versus those fed a plant diet (PD)-cotton to assess the diet-dependent expression
119 dynamics. Interestingly, *HaST46* expression was elevated exclusively in the PMG of
120 L5 larvae fed a plant diet (PD) compared to AD, whereas *HaST69* exhibited the
121 opposite trend **(Figure 1c-d)**. The presence of HaST46 in the PMG, which is a primary
122 site for nutrient absorption during active feeding, suggests its putative role in sugar
123 absorption from feed. The selective higher expression of *HaST46* in larvae consuming
124 a plant diet supports its involvement in sugar assimilation from plant (complex) food
125 materials. This further suggests that the dietary composition possibly compensates for
126 the metabolic demand.

127 **2.2. HaST46 showed a preference toward trehalose transport**

128 Functional assays with 10mM trehalose exposure to Sf9 cells overexpressing HaST46
129 revealed a significant increase in intracellular sugar accumulation in *HaST46*-
130 expressing cells compared with the vector control **(Figure 1e and f)**. LC-MS based
131 quantification revealed that *HaST46*-expressing cells accumulated ~1.5-fold more

132 trehalose relative to controls, while glucose uptake exhibited a moderate increase
133 (~1.2-fold), suggesting a trehalose preference of HaST46. Furthermore, the structural
134 alignment of HaST46 with the human GLUT1 transporter (PDB: 4PYP) showed a high
135 degree of conservation in transmembrane domain architecture **(Figure 1g)**. Molecular
136 docking studies further revealed that CYS416 and ASN312 of HaST46 formed
137 conserved hydrogen bonds with both glucose and trehalose. At the same time,
138 TRP420 and ALA193 contributed additional interactions that stabilized trehalose
139 binding **(Figure 1g)**. These findings support the hypothesis that HaST46 functions as
140 a trehalose-preferred transporter, likely contributing to sugar uptake and homeostasis
141 in *H. armigera.*

142 **2.3. Exogenous trehalose feeding upregulates *HaST46* expression and trehalose**
143 **catabolism genes in *H. armigera***

144 Upon exogenous trehalose feeding, we observed optimal growth and fitness in the
145 case of 50mM trehalose containing diet. In comparison to this, feeding with 10mM
146 trehalose doesn't showed any noteworthy physiological impact, and 100 mM trehalose
147 lead to sugar-associated toxicity **(Supplementary File S5, Figures S1 and S2)**.
148 Feeding of 50mM trehalose induced significant changes in the expression of trehalose
149 transporters (TRETs) and metabolic genes as revealed by qRT-PCR analysis.
150 *HaST46* expression was upregulated upon trehalose feeding **(Figure 2a)**. In response
151 to this, *HaTPS/TPP* were downregulated, while *HaTreh-1* showed upregulation upon
152 feeding a diet with 50mM trehalose **(Figure 2b-c)**. This alteration in the *HaTPS/TPP*
153 expression level suggests a putative reduction in the energy-intensive endogenous
154 trehalose biosynthesis and increased hydrolysis of exogenous trehalose for energy
155 needs. Notably, *HaST69* was downregulated on a 50mM TD, indicating that it is

156 potentially not involved in trehalose absorption from the gut **(Supplementary File S5,**
157 **Figure S3)**. Residual TPP activity was slightly reduced, while trehalase activity was
158 high in larvae fed the 50mM TD ($p < 0.01$) **(Figure 2d-e)**. Metabolomic quantification
159 showed that the insect fed on the trehalose-containing diet showed relatively more
160 accumulation compared to the control **(Figure 2f)**. Furthermore, increased
161 accumulation of ATP and low ADP/AMP indicates little demand for ATP hydrolysis in
162 trehalose fed insects **(Figure 2f)**.This evidence suggests a preference for hydrolytic
163 metabolism under elevated dietary trehalose, which is likely to convert absorbed
164 trehalose into glucose for systemic energy needs.

165 **2.4. *HaST46* showed gut-specific upregulation in response to trehalose feeding**

166 Tissue-specific gene expression upon 50mM trehalose feeding was further analyzed
167 to elucidate the dynamics of trehalose transport. The relative expression of *HaST46*
168 and *HaTPP* was reduced in hemolymph **(Figure 3a-b)**, while the expression of
169 *HaTreh1* and *HaTreh2* was nearly unchanged **(Figure 3c-d)**. The gut showed a
170 significant ~3-fold increase in *HaST46* expression under a 50mM TD **(Figure 3e)**,
171 indicating an increase in the need to transport and use excess trehalose in the gut
172 tissue. As the midgut is the primary site for transporter-mediated dietary trehalose
173 uptake, *HaST46* overexpression was found to be relevant. *HaTPS/TPP* expression
174 was found to be unchanged, while *HaTreh1* and *HaTreh2* expression were
175 significantly high **(Figure 3f-h)**. *HaST46* expression in the fat body (key tissue for
176 trehalose synthesis) was found to be unchanged **(Figure 3i)**. Interestingly, the
177 expression of *HaTPS/TPP* decreased significantly, suggesting a reduced endogenous
178 trehalose biosynthesis **(Figure 3j)**. *HaTreh1* and *HaTreh2* expression were relatively
179 high in the fat body of trehalose-fed insects **(Figure 3k-l)**. These observation suggests

180 that dietary trehalose downregulates internal trehalose synthesis through feedback
181 inhibition.

182 **2.5. Metabolomic Profiling Reveals Trehalose Trade-off**

183 LC-MS analysis was performed for hemolymph of insects fed on artificial diet (AD) and
184 a trehalose-rich diet (TD) to quantify systemic metabolic changes. TD-fed larvae
185 exhibited relatively elevated levels of trehalose, particularly in the hemolymph
186 **(Supplementary File_S5, Figure S5).** In addition, downstream glycolytic
187 intermediates such as glucose-6-phosphate and pyruvate were elevated, supporting
188 the notion that absorbed trehalose is rapidly catabolized into usable energy. These
189 results confirm that trehalose supplementation alters gene expression and shifts the
190 metabolic landscape toward catabolic flux, optimizing energy production in the
191 presence of abundant dietary sugar in *H. armigera.*

192 **2.6. *HaST46* knockdown induces compensatory upregulation of the trehalose**
193 **anabolism TPS/*TPP* gene**

194 RNA interference (RNAi) was employed to silence gut-prevalent *HaST46* expression.
195 We achieved ~80% reduction in the *HaST46* transcripts levels compared with the
196 empty vector **(Figure 4a)**. Notably, insects with *HaST46* silencing that were fed a 50
197 mM TD exhibited a compensatory increase in *HaST46* expression, suggesting a
198 feedback mechanism and highlighting its critical role in trehalose absorption from the
199 gut **(Figure 4b)**. Furthermore, trehalase activity was elevated in TD-fed insects
200 compared with AD-fed insects **(Figure 4c-d)**. LC-MS analysis revealed a decrease in
201 trehalose levels in the insect body upon silencing *HaST46*, indicating putative
202 involvement in the dietary trehalose absorption and resulting in an overall decrease in

203 endogenous trehalose content **(Figure. 4e)**. However, upon trehalose feeding to
204 *dsHaST46* insects, the trehalose level was almost the same as in the control **(Figure**
205 **4f)**. These findings highlight the potential role of *HaST46 in* trehalose transport. The
206 impact of *HaST46* silencing on nutritional efficiency was assessed by measuring
207 nutritional indices in both the control and silenced groups. Nutritional indices were
208 almost the same in both groups, such as the control and *HaST46* silenced insects
209 **(Supplementary File_S5, Figure S8-9)**.

210 The expression of other trehalose transporter genes (*HaST09*, *HaST29*,
211 *HaST64*, and *HaST69*) was examined in *dsHaST46*-fed larvae to explore potential
212 compensatory mechanisms. Silencing *HaST46* resulted in significant downregulation
213 of these genes, suggesting overall impact due to reduced trehalose content upon
214 silencing (Supplementary File_S5, Figure 12a). *HaST09*, *HaST29*, *HaST64*, and
215 *HaST69* exhibited upregulation in exogenous trehalose, although the functional
216 significance of these changes requires further investigation (Supplementary File_S5,
217 Figure 12b). These results underscore the pivotal role of *HaST46* in modulating
218 trehalose transport and metabolism.

219 **2.7. *HaST46* overexpression showed gut specificity and may enhance dietary**
220 **trehalose**

221 Transient overexpression of *HaST46* was confirmed with qRT-PCR analysis, showing
222 ~1000-fold higher expression of *HaST46* in treated larvae compared with the control
223 **(Figure 5a)**. *HaST46* overexpression in larvae did not significantly alter trehalase
224 activity, suggesting a maintained balance between trehalose synthesis and absorption
225 to preserve homeostasis **(Figure 5b)**. Further, we observed the upregulation of
226 *HaST46* in all three tissues of the *HaST46-OE* insects upon trehalose feeding

227 compared with the control group. Interestingly, there was a significant upregulation of
228 *HaST46* in the gut, indicating the potential preferred localization of overexpressed
229 *HaST46* in the gut tissue **(Figure 5c-e)**. However, there was a significant increase in
230 the *HaST46* transcript level in a group of insects fed on a trehalose-rich diet in the gut,
231 followed by hemolymph and fat **(Figure 5c-e)**. Trehalose levels were slightly high in
232 TD-fed *HaST46*_OE insects **(Figure 5f-g)**. At the same time, trehalase activity was
233 also found to be high in TD-fed *HaST46*_OE insects **(Figure 5h)**. These results
234 suggest that *HaST46* facilitates the uptake of dietary trehalose and reinforces its role
235 in sugar homeostasis and energy balance in Lepidopterans.

236 **3. Discussion**

237 Trehalose is key in energy homeostasis, functioning as a circulating sugar and
238 substrate for rapid energy mobilization. The identification and functional
239 characterization of *HaST46* as a trehalose-specific transporter localized to the
240 posterior midgut, principal site for nutrient uptake, highlights its putative function in
241 dietary sugar absorption **(Figure 1a and b)** (Terra et al. 2023). Furthermore, the
242 nutritionally responsive expression patterns of *HaST46* suggest that its expression is
243 coupled to the diet composition and larval metabolic demand. The higher expression
244 of *HaST46* in complex or plant diet reflects an adaptive shift to facilitate the uptake of
245 structurally and compositionally diverse carbohydrates in natural food sources **(Figure**
246 **1c and d)**. This adaptive plasticity aligns with earlier reports of the gut-specific
247 modulation of nutrient transporters in response to dietary sugars in lepidopteran larvae
248 (Azzouz et al. 2005), underscoring the ecological and physiological relevance of
249 transporter regulation in herbivorous pests.

250 The substrate preference of HaST46 for trehalose over glucose represents a
251 functional specialization **(Figure 1e and f)**. Despite structural conservation with
252 GLUT1, HaST46 exhibits trehalose preference over glucose, suggesting an
253 evolutionary divergence toward the hemolymph sugar composition of holometabolous
254 insects **(Figure 1g)**. This specificity likely enhances transport efficiency and minimizes
255 competitive inhibition, optimizing trehalose handling in sugar-rich dietary contexts.

256 At the metabolic level, the changes in trehalose biosynthesis and degradation
257 pathways in response to transporter activity reflects a coordinated homeostatic
258 system. The downregulation of endogenous trehalose synthesis in the presence of
259 abundant dietary trehalose suggests a resource-efficient switch that curtails ATP-
260 intensive biosynthesis in favour of direct absorption **(Figure 2a to e)**. Increased level
261 of ATP compared to low level of ADP/AMP suggest low demand of ATP hydrolysis in
262 exogenous supply of trehalose **(Figure 2f)**. This trade-off supports the notion that
263 insects prioritize the least metabolically costly route to meet carbohydrate
264 requirements, a trait advantageous for survival in fluctuating nutritional environments.
265 Furthermore, systemic metabolic shifts, evidenced by increased glycolytic
266 intermediates in trehalose-fed larvae, indicate that transporter-mediated uptake
267 directly fuels energy metabolism, facilitating rapid developmental transitions. This
268 catabolic reprogramming toward glucose-generating pathways mirrors the metabolic
269 flux observed during feeding stages in other insects and provides a mechanistic
270 explanation for the physiological benefits of dietary trehalose.

271 RNAi-mediated silencing reduces *HaST46* transcript abundance and triggers
272 compensatory responses at both transcriptomic and enzymatic levels **(Figure 4a and**
273 **b)**. Trehalose biosynthetic genes upregulation on *HaST46* knockdown implies

274 compensation for decreased absorption by enhancing endogenous production.
275 However, the simultaneous downregulation of other transporter isoforms suggests a
276 response to reduced overall trehalose levels. Notably, despite transporter knockdown,
277 nutritional indices remained relatively unaffected, indicating that *H. armigera* maintains
278 systemic metabolic resilience, likely through alternative sugar transporters or
279 compensatory physiological mechanisms. Conversely, *HaST46* overexpression did
280 not disrupt homeostasis, suggesting that while the transporter enhances trehalose
281 uptake, the system possesses regulatory checkpoints that prevent metabolic overload
282 **(Figure 5a and b)**.

283 Together, these findings highlight role of *HaST46* in trehalose acquisition and
284 regulation. Its dynamic expression, functional specificity, and involvement in feedback-
285 controlled metabolic shifts position it as a key mediator of dietary sugar assimilation.
286 Given that trehalose metabolism is unique to insects and absent in vertebrates,
287 *HaST46* offers a promising molecular target for the selective disruption of energy
288 metabolism in lepidopteran pests.

289 4. Materials and Methods

290 4.1 Differential gene expression and proteomic signature analysis

291 Publicly available *H. armigera* gut transcriptomic and proteomic datasets (Ioannidis et
292 al. 2022) were used for expression profiling of *HaSTs*. Out of 5 tissue specific *HaSTs*,
293 only *HaST46* and *HaST6*9 were mapped to gut transcriptomics and proteomics. For
294 transcriptomics, raw fragments per kilobase of transcript per million mapped reads
295 (FPKM) values were extracted, $\log_2(x+1)$ transformed, and row-wise Z-score
296 normalized before hierarchical clustering using Euclidean distance and complete

297 linkage in the pheatmap package (R v4.x). For proteomics, the absence or presence
298 of HaSTs in the proteomics set was denoted in binary form. Heatmaps were generated
299 using TBtools 1.09 (Chen et al. 2020) to visualise stage- and tissue-specific
300 expression patterns. For bar plots, mean FPKM values ± SEM were calculated across
301 biological replicates.

302 **4.2 *HaST46* overexpression in Sf9 cells**

303 For overexpression, *HaST46* was cloned into the pIBV5 vector and sequence-
304 confirmed. Sf9 cells (4×10^6) were seeded in a T25 cell culture flask (Corning, NY,
305 USA) with 1 mL serum-free SF900 II SFM media (Thermo Scientific, Waltham, MA,
306 USA) and allowed to adhere by incubating for 30 minutes at 27 °C. For transfection,
307 1.5 µg of either the EGFP_pIBV5 control plasmid or the *HaST46-pIBV5* plasmid was
308 diluted in 100 µL SF-900 II SFM (without antibiotics). Separately, 8µL Cellfectin II
309 reagent (Gibco, Waltham, MA, USA) was diluted in 100 µL Sf-900 II SFM and
310 incubated for 30 minutes. The DNA and lipid solutions were combined (total 200 µL)
311 and incubated for an additional 30 min to allow complex formation. The transfection
312 mix was added dropwise while gently rocking the flask for an even distribution. Flasks
313 were incubated for 5-7 hours at 27°C. After the incubation, the media was removed,
314 and fresh Sf-900 II SFM containing blasticidin (Gibco, Waltham, MA, USA) antibiotic
315 was added and incubated for 48 hours. Overexpression was confirmed by qRT-PCR.
316 For the sugar uptake assay, 5mM and 10mM concentrations of glucose and trehalose
317 were added to the media, and the cells were incubated for varying time points (0, 5,
318 and 10 minutes). Following incubation, the media and cells were collected for
319 metabolite extraction and analysis. Sugar uptake was determined from changes in
320 extracellular and intracellular sugar concentrations by metabolite profiling.

321 **4.3 Structural modelling and docking**

322 Three dimensional structure of HaST46 was predicted using Alphafold 3 server
323 (https://alphafoldserver.com/). Structural aligment of best model was performed using
324 PyMol (The PyMOL Molecular Graphics System, Version 3.0 Schrödinger, LLC.) using
325 Human Glut1 (PDB ID: 4PYP) structure as reference. Binding site residues of Glut1
326 were used to predict the binding pocket of HaST46 and molecular docking of glucose
327 and trehalose was performed using AutoDock Tool as described earlier (Barbole et al.
328 2024).

329 **4.4 Quantitative Real-Time PCR (qRT-PCR) Analysis**

330 Total RNA was extracted from 80–100 mg of insect cells/tissues using the TRIzol
331 reagent (Invitrogen, Waltham, MA, USA). To eliminate DNA contamination, RNA was
332 treated with RQ1 RNase-free DNase. First-strand cDNA was synthesised from 5 µg
333 RNA using oligo-dT primers and the High-Capacity cDNA Reverse Transcription Kit
334 (Applied BioSystem, Foster, CA, USA), following the manufacturer's protocol. Gene
335 expression was quantified using a 7500 Fast Real-Time PCR System (Applied
336 Biosystems, Foster, CA, USA) with Takara TB Green Premix Ex Taq II. Primer list
337 provided in supplementary information (S3). Expression dynamics, including transcript
338 abundance (2-ΔCt) and fold change (2-ΔΔCt), were visualised using GraphPad
339 software. The expression of five *HaSTs*, *trehalose-6-phosphate synthase* (*TPS*),
340 *trehalose-6-phosphate phosphatase* (*TPP*), and trehalase was assessed in trehalose-
341 fed tissues, with the gut as the reference for fold change in fifth instar larvae. *HaSTs*
342 expression was further evaluated in haemolymph, fat body, and silencing assays,
343 using control expression as the reference.

344 **4.5 Metabolite Analysis Using LC-Orbitrap-MS**

345 To extract metabolites, 80-100mg of finely crushed sample powder was mixed with
346 500 µL of 80% MS-grade methanol to ensure efficient metabolite extraction (J.T.
347 Baker, Center Valley, PA, USA). Methods were carried out according to the
348 procedures described in the supplementary method 4.

349 **4.6 Insect rearing**

350 Larval populations of *H. armigera* were obtained from the ICAR-National Bureau of
351 Agricultural Insect Resources (NBAIR), Bengaluru, India, and maintained on a
352 chickpea-based artificial diet (AD) for multiple generations. Insects were reared at 25
353 ± 1°C, 70 ± 10% relative humidity, and a 16:8 h light: dark photoperiod. Adult mating
354 boxes, containing equal numbers of males and females, were provided with 10% (w/v)
355 sucrose solution and 1% (w/v) vitamin E, with a muslin cloth for egg collection (Dawkar
356 et al. 2016).

357 **4.7 Exogenous trehalose feeding and tissue collection for the bioassay**

358 For exogenous trehalose feeding in the *H. armigera* bioassay, freshly moulted second
359 instar larvae were fed AD supplemented with 10mM, 50mM, or 100mM trehalose for
360 6 days to assess the impact on nutritional indices efficiency of conversion of ingested
361 food (ECI), efficiency of conversion of digested food (ECD), and approximate
362 digestibility (AD) and expression of sugar transporter genes (*HaSTs*). Three biological
363 replicates (n = 10 larvae each) were used, and the samples were flash-frozen in liquid
364 nitrogen and stored at -80°C. For tissue collection, fifth instar larvae were starved for
365 1-2 hours followed by washing with phosphate-buffered water and dissected under
366 RNase-free conditions to collect haemolymph, gut tissues (foregut, midgut, hindgut),
367 and fat body. The samples were flash-frozen and stored at -80°C.

368 **4.8 In vitro Targeted Putative Sugar Transporter Gene *HaST46* Silencing via**
369 **dsRNA Feeding**

370 Silencing of *the HaST46* gene was performed using microbial-based dsRNA
371 production. To generate dsRNA targeting *HaST46*, a 400-bp fragment was PCR
372 amplified using Phusion DNA Polymerase (Thermo Fisher Scientific, Waltham, MA,
373 USA) and a Proflex PCR machine (Thermo Fisher Scientific, Waltham, MA, USA) with
374 primers (**Supplementary File S3)**. Detailed methods are provided in **Supplementary**
375 **method 2**.

376 **4.9 Transient overexpression of *HaST46***

377 For overexpression, *HaST46* was cloned into the pIB/V5 vector (Thermo Fisher
378 Scientific, Waltham, MA, USA) and sequence-verified. Larvae were starved for 3 h
379 before injection. Further process were carried out according to the procedures
380 described in the supplementary method 3. A mixture of 1500 ng of each plasmid and
381 lipofectamine (Invitrogen, Thermo Fisher Scientific Inc., Waltham, MA, USA) (1:1 v/v),
382 incubated for 30 minutes, was injected into the haemocoel between the 5th and 7th
383 abdominal segments. The EGFP pIB/V5 plasmid served as the control (Barbole et al.
384 2024).

385 **4.10 Enzymatic activity**

386 The α,α-trehalase activity was determined by measuring the amount of glucose
387 released from the hydrolysis of α,α-trehalose using the dinitrosalicylic acid (DNSA)
388 reagent (Sigma-Aldrich, Merck KGaA, St. Louis, MO, USA). By monitoring the release
389 of inorganic phosphate (Pi) from the crude extract using the malachite-green reagent
390 (Sigma-Aldrich, St. Louis, MO, USA) to assess the enzymatic activity of trehalose 6-

391 phosphate phosphatase (TPP). The assay was conducted following the modified
392 protocol of (Klutts et al. 2003). Methods were performed as described in
393 Supplementary method 4b.

394 **4.11 Statistical analysis**

395 All experiments contain 3 or more biological replicates. Data were expressed as mean
396 ± SE using GraphPad Prism v8.0 (GraphPad Software, San Diego, CA, USA). The
397 unpaired Student's t-test. Asterisks indicate significant changes compared to control
398 (*P-value < 0.05; **P-value < 0.01; ***P-value < 0.001, ****P-value < 0.0001).

399 **Declaration of competing interests**

400 The authors have no competing interests of a financial or personal nature.

401 **Acknowledgments**

402 Fellowship support from CSIR-UGC-NET to BYC and VJN is acknowledged. ANRF
403 (GAP336726) partially supports this work.

404 **Contributions**

405 BYC designed and conducted the experiments, performed data curation, formal
406 analysis, validation, and visualisation, and wrote and edited the original draft. VJN
407 performed only transfection in the Sf9 cell line, whereas cloning, qRT, LC-MS sample
408 preparation, and data analysis were performed by BYC. VTB carried out LC-MS
409 experiments, and RSJ performed the analysis. RSJ conceptualisation, experiment
410 design, supervision, provision of resources, funding acquisition, investigation,
411 visualisation, docking, and methodology. BYC, VTB, and RSJ contributed to writing
412 and revising the manuscript and approved the final version.

413 **Data availability statement**

414 Data are available in the figures of the article and its supplementary materials.

415 **Conflict of interest**

416 The authors declare that they have no conflicts of interest.

417

418 **References:**

419 Feofilova EP, Usov AI, Mysyakina IS, Kochkina GA. 2014. Trehalose: Chemical
420 structure, biological functions, and practical application. Microbiology. 83:184–194

421 Thorat LJ, Gaikwad SM, Nath BB. 2012. Trehalose as an indicator of desiccation
422 stress in Drosophila melanogaster larvae: a potential marker of anhydrobiosis.
423 Biochem Biophys Res Commun. 419(4):638–642

424 Zhang D-W et al. 2019. Insect behavior and physiological adaptation mechanisms
425 under starvation stress. Front Physiol. 10:163

426 Becker A, Schlöder P, Steele JE, Wegener G. 1996. The regulation of trehalose
427 metabolism in insects. Experientia. 52:433–439

428 Matsushita R, Nishimura T. 2020. Trehalose metabolism confers developmental
429 robustness and stability in Drosophila by regulating glucose homeostasis. Commun
430 Biol. 3(1):170

431 Nishimura T. 2020. Feedforward regulation of glucose metabolism by steroid
432 hormones drives a developmental transition in Drosophila. Curr Biol. 30(18):3624–
433 3632

434 Murphy TA, Wyatt GR. 1965. The enzymes of glycogen and trehalose synthesis in
435 silk moth fat body. J Biol Chem. 240(4):1500–1508

436 Shukla E, Thorat LJ, Nath BB, Gaikwad SM. 2015. Insect trehalase: physiological
437 significance and potential applications. Glycobiology. 25(4):357–367

438 Tellis MB, Kotkar HM, Joshi RS. 2023. Regulation of trehalose metabolism in

439 insects: from genes to the metabolite window. Glycobiology. 33(4):262–273

440 Tellis MB, Chaudhari BY, et al. 2023. Trehalose transporter-like gene diversity and
441 dynamics enhances stress response and recovery in Helicoverpa armigera. Gene.
442 862:147259

443 Koyama T, Texada MJ, Halberg KA, Rewitz K. 2020. Metabolism and growth
444 adaptation to environmental conditions in Drosophila. Cell Mol Life Sci. 77(22):4523–
445 4551

446 Raubenheimer D, Jones SA. 2006. Nutritional imbalance in an extreme generalist
447 omnivore: tolerance and recovery through complementary food selection. Anim
448 Behav. 71(6):1253–1262

449 Smith RL, Soeters MR, Wüst RCI, Houtkooper RH. 2018. Metabolic flexibility as an
450 adaptation to energy resources and requirements in health and disease. Endocr
451 Rev. 39(4):489–517

452 Chown SL, Gaston KJ. 1999. Exploring links between physiology and ecology at
453 macro-scales: the role of respiratory metabolism in insects. Biol Rev. 74(1):87–120

454 Miyamoto T, Amrein H. 2017. Gluconeogenesis: An ancient biochemical pathway
455 with a new twist. Fly (Austin). 11(3):218–223

456 Izadi H. 2025. Endocrine and enzymatic shifts during insect diapause: a review of
457 regulatory mechanisms. Front Physiol. 16:1544198

458 Thompson SN. 2003. Trehalose—the insect ‘blood’sugar. Adv In Insect Phys.
459 31(Supplement C):205–285

460 Al Hinai MS, Rehman A, Siddique KHM, Farooq M. 2025. The Role of Trehalose in
461 Improving Drought Tolerance in Wheat. J Agron Crop Sci. 211(3):e70053

462 Kikawada T et al. 2007. Trehalose transporter 1, a facilitated and high-capacity
463 trehalose transporter, allows exogenous trehalose uptake into cells. Proc Natl Acad
464 Sci U S A. 104(28):11585–11590. https://doi.org/10.1073/pnas.0702538104

465 Wyatt GR. 1967. The Biochemistry of Sugars and Polysaccharides in Insects. Adv In
466 Insect Phys. 4(C):287–360. https://doi.org/10.1016/S0065-2806(08)60210-6

467 Leyria J, Orchard I, Lange AB. 2020. What happens after a blood meal? A
468 transcriptome analysis of the main tissues involved in egg production in Rhodnius
469 prolixus, an insect vector of Chagas disease. PLoS Negl Trop Dis. 14(10):e0008516

470 Huang J-H, Jing X, Douglas AE. 2015. The multi-tasking gut epithelium of insects.
471 Insect Biochem Mol Biol. 67:15–20

472 Chaudhari BY, Pradhan AG, Joshi RS. 2025. Metabolic gatekeepers: Dynamic roles
473 of sugar transporters in insect metabolism and physiology. Insect Mol Biol. 34(1):1–
474 18

475 Wang X, Li E, Chen L. 2016. A review of carbohydrate nutrition and metabolism in
476 crustaceans. N Am J Aquac. 78(2):178–187

477 Riera CE, Merkwirth C, De Magalhaes Filho CD, Dillin A. 2016. Signaling networks
478 determining life span. Annu Rev Biochem. 85(1):35–64

479 Danks H V. 2007. The elements of seasonal adaptations in insects. Can Entomol.
480 139(1):1–44

481 Riaz S et al. 2021. A review on biological interactions and management of the cotton
482 bollworm, Helicoverpa armigera (Lepidoptera: Noctuidae). J Appl Entomol.
483 145(6):467–498

484 Dawkar V V. et al. 2016. The expression of proteins involved in digestion and
485 detoxification are regulated in Helicoverpa armigera to cope up with chlorpyrifos
486 insecticide. Insect Sci. 23(1):68–77. https://doi.org/10.1111/1744-7917.12177

487 Guan L et al. 2024. The Role of TcCYP6K1 and TcCYP9F2 influences trehalose
488 metabolism under high-CO2 stress in Tribolium castaneum (Coleoptera). Insects.
489 15(7):502

490 Tian Z et al. 2025. Trehalose metabolism mediates trade-offs between reproduction
491 and survival in beet webworm, Loxostege sticticalis, under heat stress. Pest Manag
492 Sci. 81(2):903–911

493 Zhou Y-F et al. 2023. Characterization of the TcCYPE2 gene and its role in
494 regulating trehalose metabolism in response to high CO2 stress. Agronomy.
495 13(9):2263

496 Ioannidis P et al. 2022. A spatiotemporal atlas of the lepidopteran pest Helicoverpa
497 armigera midgut provides insights into nutrient processing and pH regulation. BMC
498 Genomics. 23(1):75

499 Barbole RS et al. 2024. Chitinase inhibition induces transcriptional dysregulation
500 altering ecdysteroid-mediated control of Spodoptera frugiperda development.
501 Iscience. 27(3)

502 Terra WR, Ferreira C, Silva CP. 2023. Overview of insect midgut function. In:

503 Molecular physiology and evolution of insect digestive systems. Springer; p 13–26

504 Azzouz H et al. 2005. Effects of plant protease inhibitors, oryzacystatin I and
505 soybean Bowman–Birk inhibitor, on the aphid Macrosiphum euphorbiae (Homoptera,
506 Aphididae) and its parasitoid Aphelinus abdominalis (Hymenoptera, Aphelinidae). J
507 Insect Physiol. 51(1):75–86

508 Chen C et al. 2020. TBtools: an integrative toolkit developed for interactive analyses
509 of big biological data. Mol Plant. 13(8):1194–1202

510 Klutts S et al. 2003. Purification, cloning, expression, and properties of mycobacterial
511 trehalose-phosphate phosphatase. J Biol Chem. 278(4):2093–2100

512

513

514 **Figure Legends**

515 **Figure 1. Spatial expression and functional characterisation of *HaST46*** (a) Pro-
516 tein abundance across larval stages (L2, L3, L4) and gut regions (FG: foregut; AMG:
517 anterior midgut; MMG: median midgut; PMG: posterior midgut; HG: hindgut) in L5 lar-
518 vae reared on an artificial diet. (b) DGE patterns comparing larvae fed on an artificial
519 diet and a plant-based diet (cotton) across different gut compartments.
520 (c, d) Expression levels of *HaST46* and *HaST69* in the posterior midgut under the two
521 dietary regimes. Data represent mean ± SEM of biological replicates. Statistical signif-
522 icance was determined using an unpaired *t*-test ($P < 0.05$). (e) Verification of *HaST46*
523 overexpression by qRT-PCR. (f) Quantification of D-glucose and trehalose in cell su-
524 pernatants and lysates using LC–MS/MS after supplementation of the culture medium
525 with glucose (5 mM, 10 mM) or trehalose (5mM, 10mM) at 0, 5, and 10 min intervals.
526 All data are presented as mean ± SEM. Statistical analysis was performed using an
527 unpaired *t*-test ($P < 0.05$). (g) Structural conservation of HaST46 with human GLUT1
528 transporter. Molecular interaction of HaST46 with glucose and trehalose.

529 **Figure 2. Gene expression and enzymatic activity upon exogenous trehalose**
530 **feeding in *H. armigera*.** (a–c) qRT-PCR analysis of *HaST46* and trehalose metabo-
531 lism-related genes following dietary trehalose supplementation. Transcript abundance
532 was normalised to reference genes and expressed as fold change ($2^{-\Delta\Delta Ct}$).
533 (d, e) In vivo activity of trehalase and trehalose-6-phosphate phosphatase (TPP) in
534 larvae fed a 50mM trehalose-enriched diet or an artificial diet.
535 (f) Quantification of trehalose, ATP, ADP and, AMP in whole larvae using LC–MS un-
536 der the same dietary conditions. Data are presented as mean ± SEM, with statistical
537 significance assessed by an unpaired *t*-test ($P < 0.05$).

538 **Figure 3. Tissue-specific expression of *HaST46* and trehalose metabolism genes**
539 **following trehalose feeding.** (a–c) qRT-PCR analysis showing expression patterns
540 in haemolymph, fat body, and gut tissues. Transcript levels were normalised to refer-
541 ence genes and expressed as fold change ($2^{-\Delta\Delta Ct}$) relative to control.
542 Data represent mean ± SEM, with statistical differences determined by an unpaired *t*-
543 test ($P < 0.05$).

544 **Figure 4. Silencing of *HaST46* in *H. armigera*.** (a, b) qRT-PCR analysis of *HaST46*
545 expression in whole-body samples from control insects (empty L4440 vector) and
546 dsRNA-treated insects, either fed on an artificial diet or an artificial diet supplemented
547 with 50mM trehalose. (c, d) In vivo trehalase and TPP activities under the same con-
548 ditions. (e, f) Trehalose levels quantified in whole insects using LC–MS/MS.
549 All values are mean ± SEM, with statistical analysis performed using an unpaired *t*-
550 test ($P < 0.05$).

551 **Figure 5. Overexpression of *HaST46* in fifth instar larvae of *H. armigera*.**
552 (a) qRT-PCR expression of *HaST46* in whole-body (b) In vivo trehalase activity in
553 whole-body samples following *HaST46* overexpression. (c-e) Expression analysis of
554 *HaST46* in haemolymph, fat body, and gut tissues under four feeding conditions: arti-
555 ficial diet, trehalose-rich diet (50mM), *HaST46* overexpression with artificial diet, and
556 *HaST46* overexpression with trehalose-rich diet (50mM). Transcript levels were nor-
557 malised to reference genes and expressed as fold change ($2^{-\Delta\Delta Ct}$). (f-g) LC–MS/MS-
558 based quantification of trehalose in haemolymph after *HaST46* overexpression. (h) In
559 vivo trehalase activity in in haemolymph, fat body, and gut tissues samples following
560 *HaST46* overexpression. Data are shown as mean ± SEM, with significance assessed
561 using an unpaired *t*-test ($P < 0.05$).

562 **Supplementary information**

563 **Supplementary information S1**: H. armigera STs gene sequences

564 **Supplementary information S2:** Name of putative HaSTs and its corresponding
565 gene id from NCBI gene database and scaffold id from transcriptome data

566 **Supplementary information S3:** HaST primers used for real-time PCR analysis and
567 silencing experiment

568 **Supplementary information S4:** General methods for real-time PCR, TPP and tre-
569 halase enzymatic acitivites.

570 **Supplementary information S5:** *H. armigera* growth and phenotype upon silencing
571 and upregulation. Also real-time expression analysis of HaSTs related.

572

Figure 1

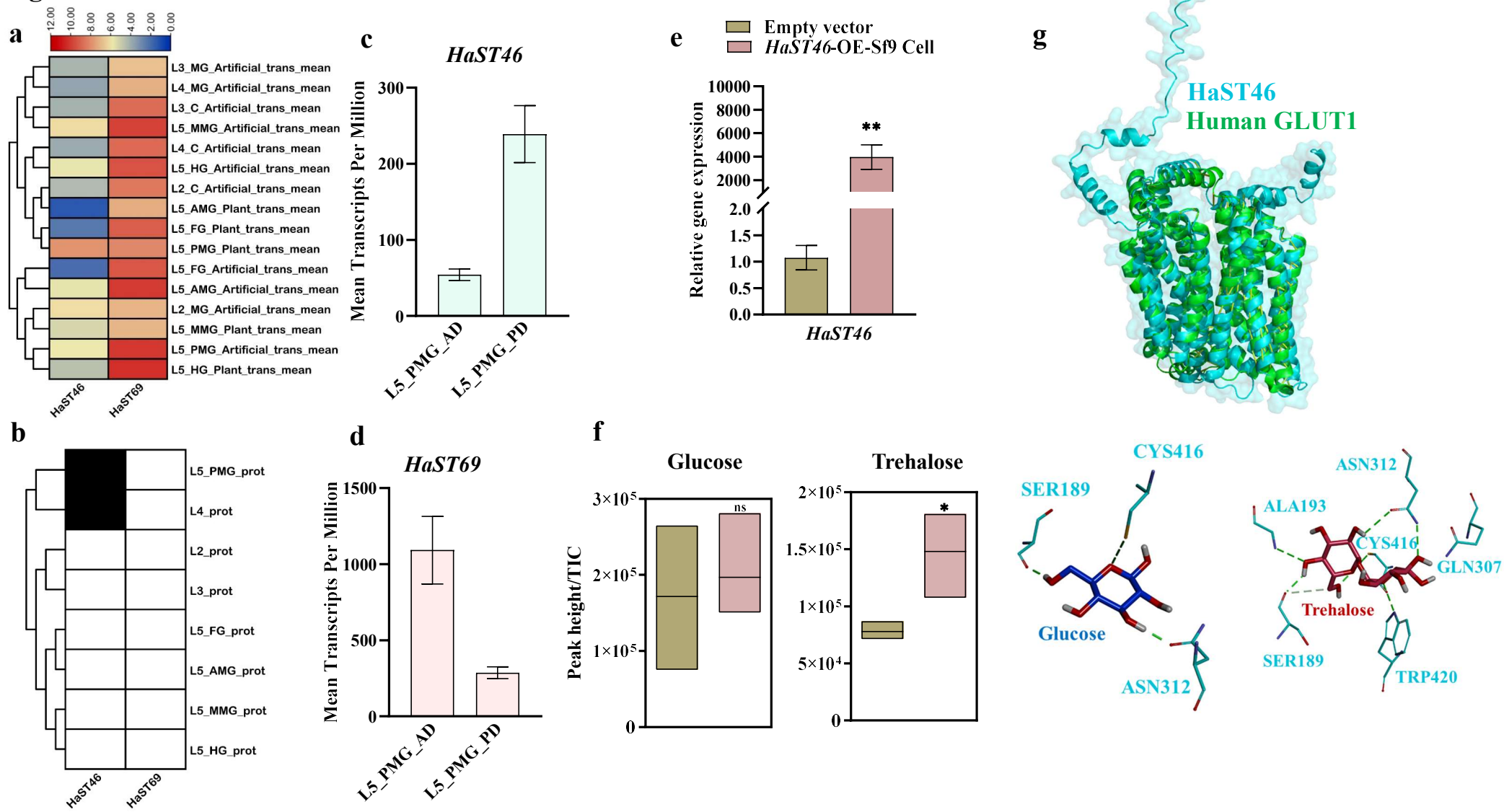
a
12.00
10.00
8.00
6.00
4.00
2.00
0.00
L3_MG_Artificial_trans_mean
L4_MG_Artificial_trans_mean
L3_C_Artificial_trans_mean
L5_MMG_Artificial_trans_mean
L4_C_Artificial_trans_mean
L5_HG_Artificial_trans_mean
L2_C_Artificial_trans_mean
L5_AMG_Plant_trans_mean
L5_FG_Plant_trans_mean
L5_PMG_Plant_trans_mean
L5_FG_Artificial_trans_mean
L5_AMG_Artificial_trans_mean
L2_MG_Artificial_trans_mean
L5_MMG_Plant_trans_mean
L5_PMG_Artificial_trans_mean
L5_HG_Plant_trans_mean
HaST46
HaST69
b
L5_PMG_prot
L4_prot
L2_prot
L3_prot
L5_FG_prot
L5_AMG_prot
L5_MMG_prot
L5_HG_prot
HaST46
HaST69
c
HaST46
Mean Transcripts Per Million
300
200
100
0
L5_PMG_AD
L5_PMG_PD
d
HaST69
Mean Transcripts Per Million
1500
1000
500
0
L5_PMG_AD
L5_PMG_PD
e
Empty vector
HaST46-OE-Sf9 Cell
Relative gene expression
10000
8000
6000
4000
2000
2.0
1.5
1.0
0.5
0.0
**
HaST46
f
Glucose
Trehalose
Peak height/TIC
3×10^5
2×10^5
1×10^5
0
ns
2×10^5
1.5×10^5
1×10^5
5×10^4
0
*
g
HaST46
Human GLUT1
CYS416
SER189
Glucose
ASN312
ASN312
ALA193
CYS416
GLN307
Trehalose
SER189
TRP420

Figure 2

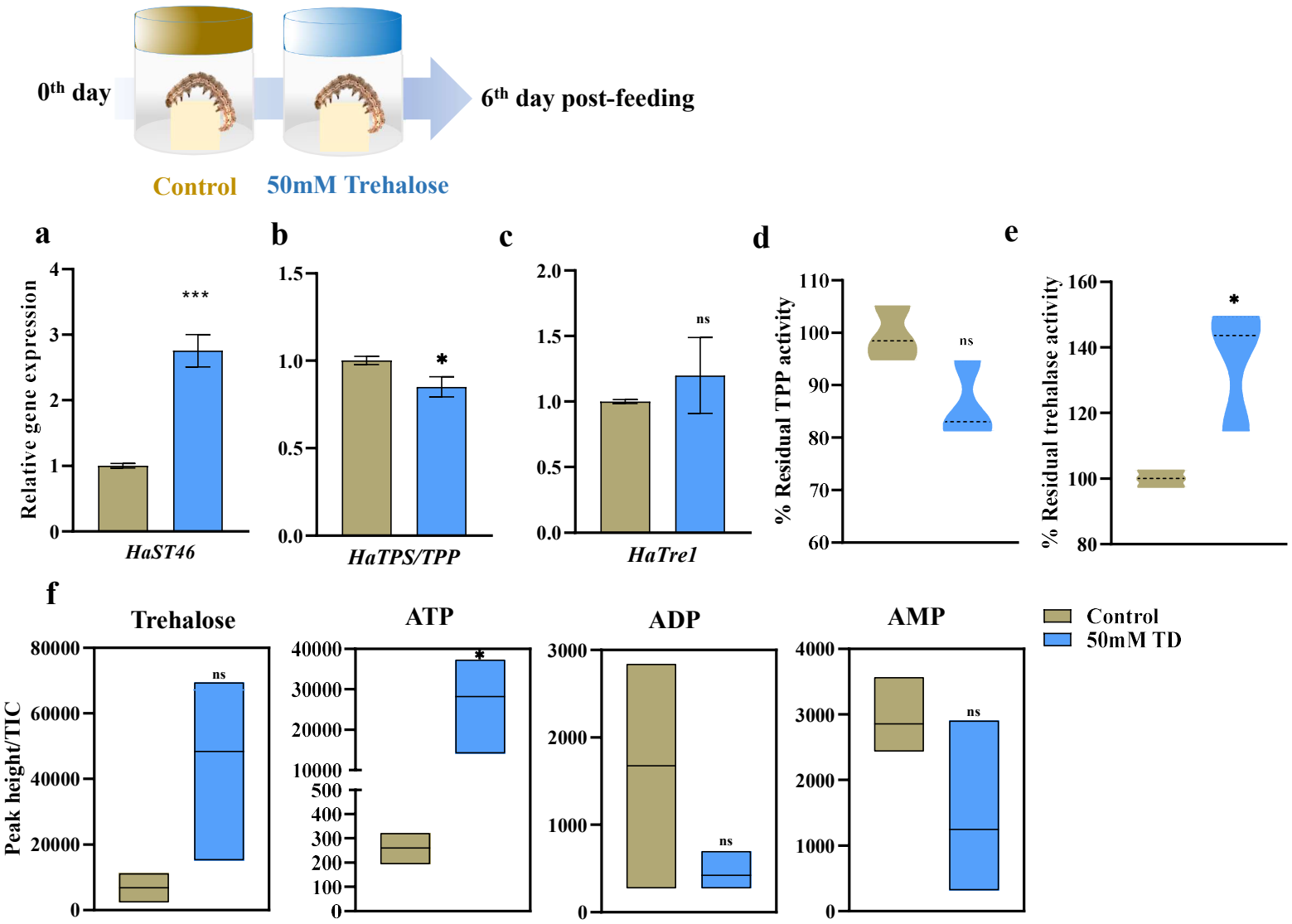
0th day
6th day post-feeding
Control
50mM Trehalose
a
Relative gene expression
HaST46
b
HaTPS/TPP
c
HaTre1
d
% Residual TPP activity
e
% Residual trehalase activity
f
Trehalose
ATP
ADP
AMP
Peak height/TIC
Control
50mM TD
ns
*
***

Figure 3

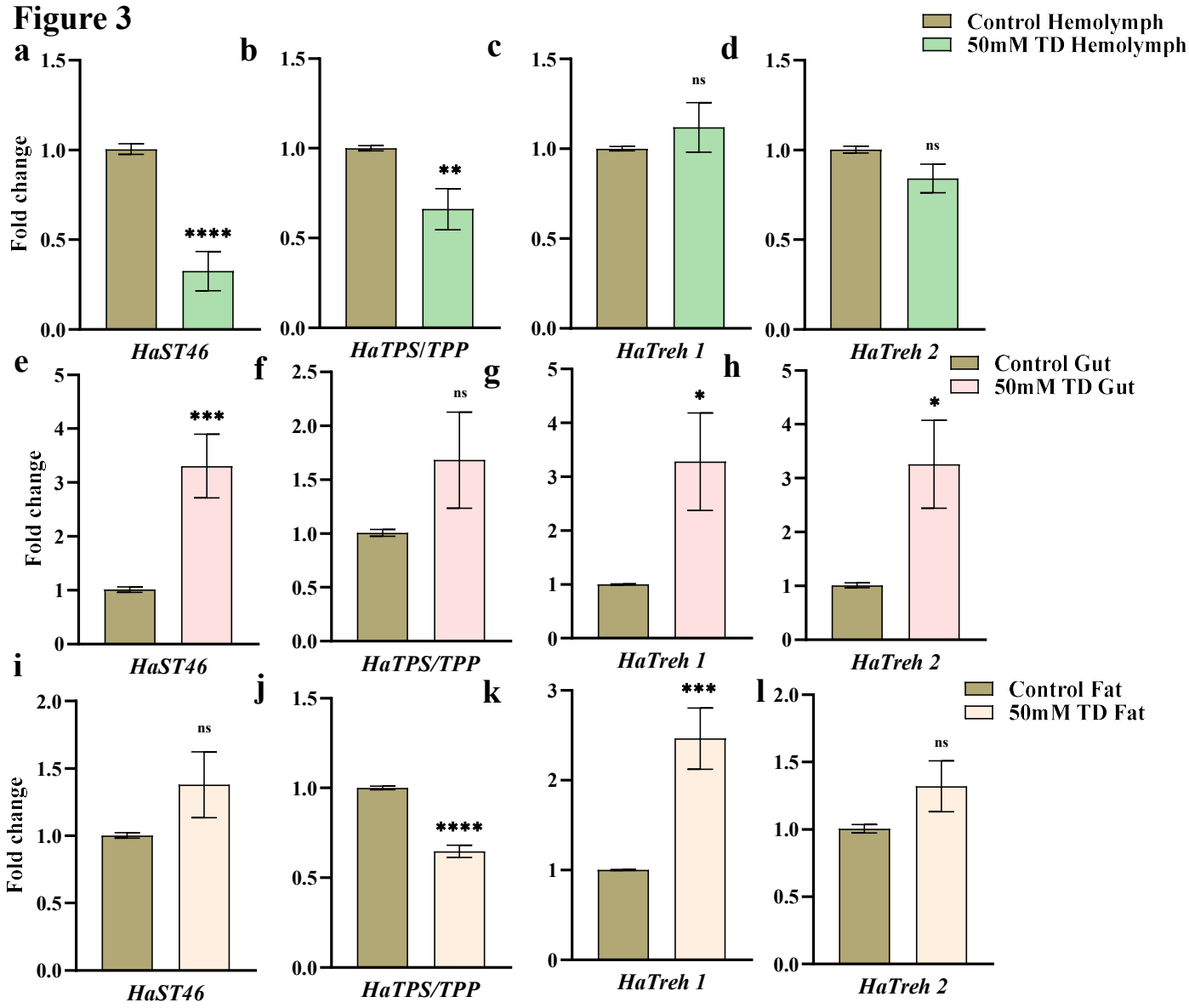
Control Hemolymph
50mM TD Hemolymph
Control Gut
50mM TD Gut
Control Fat
50mM TD Fat
Fold change
a
b
c
d
e
f
g
h
i
j
k
l
HaST46
HaTPS/TPP
HaTreh 1
HaTreh 2
****
**
ns
***
*

Figure 4

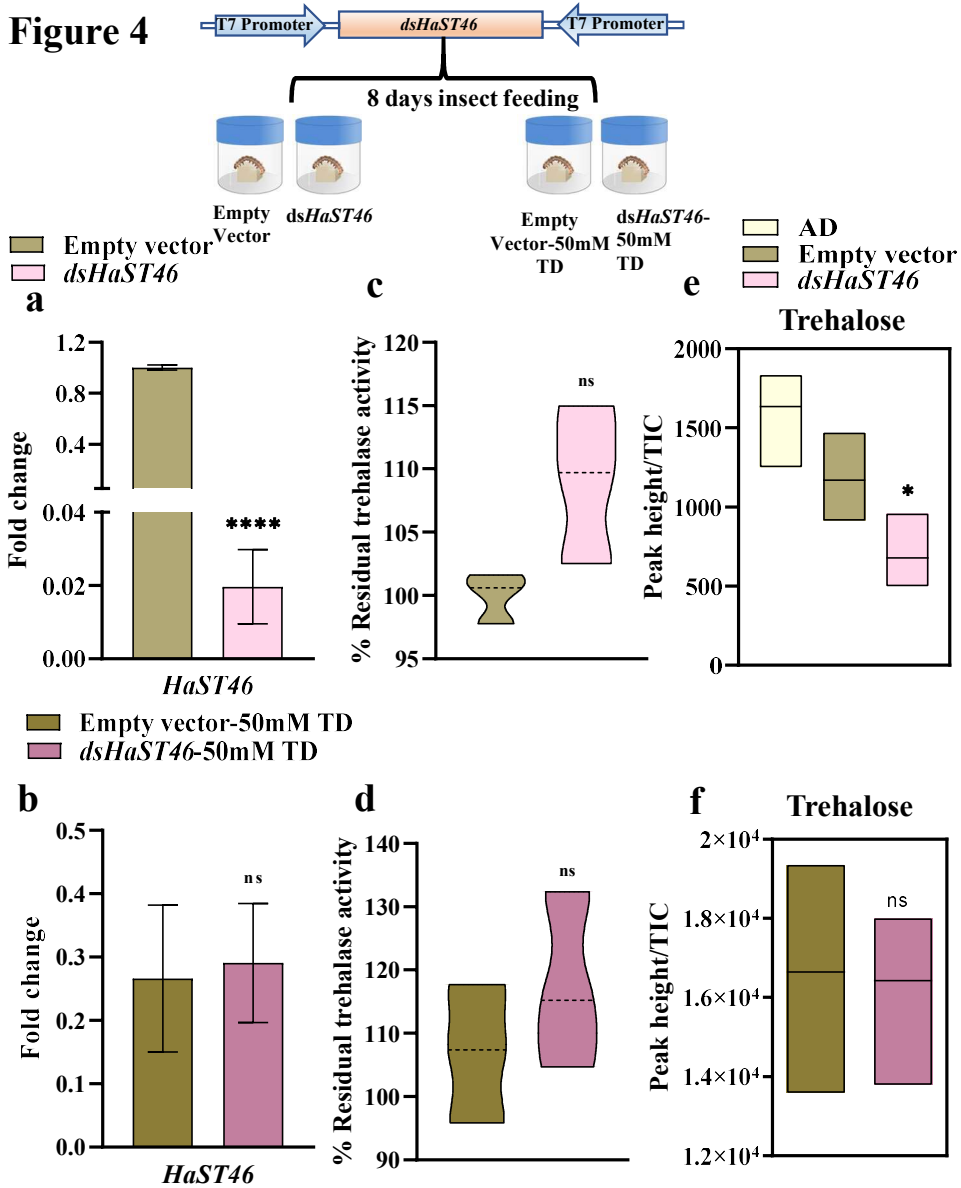
T7 Promoter
dsHaST46
T7 Promoter
8 days insect feeding
Empty Vector
dsHaST46
Empty Vector-50mM TD
dsHaST46-50mM TD
Empty vector
dsHaST46
AD
Empty vector
dsHaST46
a
Fold change
****
HaST46
c
% Residual trehalase activity
ns
e
Trehalose
Peak height/TIC
*
Empty vector-50mM TD
dsHaST46-50mM TD
b
Fold change
ns
HaST46
d
% Residual trehalase activity
ns
f
Trehalose
Peak height/TIC
ns

Figure 5

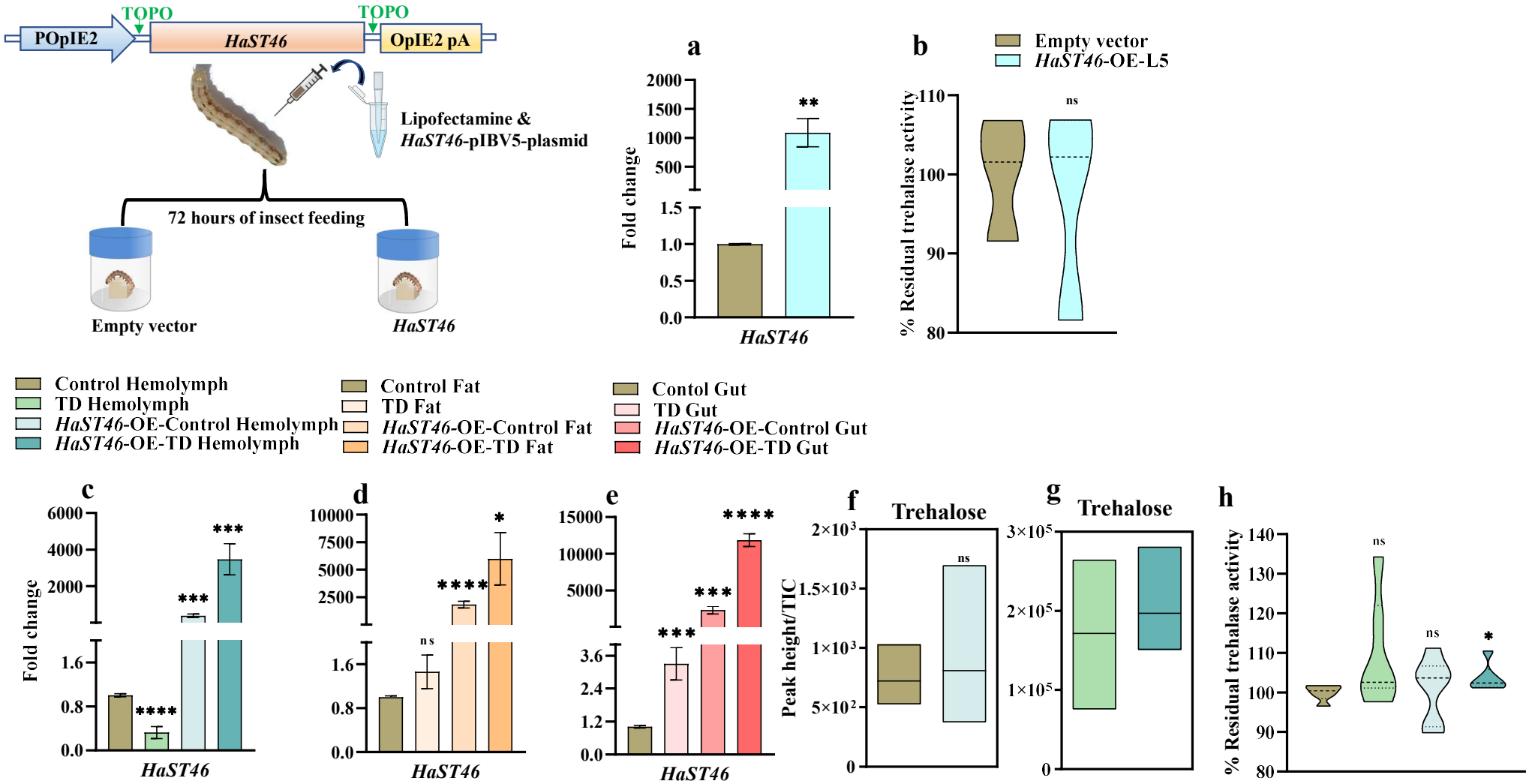
TOPO
TOPO
POpIE2
HaST46
OpIE2 pA
Lipofectamine &
HaST46-pIBV5-plasmid
72 hours of insect feeding
Empty vector
HaST46
a
Fold change
HaST46
b
Empty vector
HaST46-OE-L5
% Residual trehalase activity
ns
Control Hemolymph
TD Hemolymph
HaST46-OE-Control Hemolymph
HaST46-OE-TD Hemolymph
Control Fat
TD Fat
HaST46-OE-Control Fat
HaST46-OE-TD Fat
Contol Gut
TD Gut
HaST46-OE-Control Gut
HaST46-OE-TD Gut
c
d
e
f
Trehalose
Peak height/TIC
g
Trehalose
h
% Residual trehalase activity